

Deposition and erosion-corrosion rippling in boiler tubes

W. M. M. Huijbregts

Kema Scientific & Technical Reports 3 (2): 33-41 (1985), ISSN 0167-8590; ISBN 90-353-0025-4.

Abstract

Rippling in high-pressure boiler tubes increases flow resistance; rippling is caused by too high water-flow velocities. Experiments were carried out at the KEMA experimental boiler installation. The effects studied were those of heat load, tube wall thickness, presence of a casing and chemical composition of the steel.

Two types of experiments were carried out, one under supercritical conditions and one under subcritical two-phase (water-steam) flow conditions. Two types of rippling appeared to occur:

1. deposition rippling: ripples are formed since magnetite crystals are arranged in a ripple pattern;
2. erosion-corrosion rippling: the steel surface itself is erosion-corroded into a ripple pattern.

1. Introduction

High-pressure boilers have come into operation in the last fifteen years. Increasing flow resistance is sometimes observed in those boilers, resulting in a lower boiler efficiency. In 1968 Grosskraftwerk Mannheim (GKM) started a detailed research project on operational boiler tubes (Schuster, 1971; Schoch et al., 1972). A few years later, the University of Stuttgart joined GKM in a study in greater depth the results of which have in the meantime been published (Pfau et al., 1978).

In the German study flow resistance had increased to approx. 50% due to rippling in the oxide layer on the tube wall across the direction of flow. Ripple height was 1-5 ltm and ripple intervals were 30-100 pm. Ripples in the samples appeared as undulations in the oxide layer. The steel oxide front was straight and there was no corrosion below the thinner oxide areas.

KEMA has started a program to complement the German research and focuses on the effects of steel quality and heat flux. One experiment was done under supercritical and one under subcritical conditions. Because of experience gained from the German studies, a variety of steel and tube types were used.

2. Experimental set-up



Figure 1. Experimental boiler installation at KEMA.

Figure 1 shows the KEMA experimental boiler installation. The test conditions are presented in Table 1. A supercritical pressure of 25 MPa and a temperature of 613 K were chosen for the first experiment. According to the GKM results, very noticeable ripple oxide structures form under those conditions. A pressure of 18 MPa and a steam fraction of 0.95 chosen for the second experiment because little was known about the influence of two-phase flow upon rippling. The tubes tested are shown in Figures 2 and 3.

Table 1. Data from the two experiments with the KEMA experimental boiler.

Exposure number	Exposure data		Test tubes (each 1.5 m long)	
	1	Pressure (Mpa)	25	1A
Temperature (K)		613	1B	Tube with 5 welded segments for heat load tests
Water flow (m/s)		10.5	1C	Tube with 3 welded segments, each one turned off externally to 3 different wall thicknesses
Water conditioning		NH3	1D	Cased tube with 5 welded segments; two holes drilled in the inner tube, which provided access of boiler water to casing
pH		9.2		
Exposure time (h)		500		
2	Pressure (Mpa)	18	2E	14Mn4 tube, a 40 cm length of which was heat-loaded
	Temperature (K)	628		
	Water flow (m/s)	10.5	2E	15Mo3 tube, an 80 cm length of which was heat-loaded
	Water conditioning	NH3		
	pH	9.2	2A	Tube consisting of 13 welded segments
	Steam fraction	0.95		
	Exposure time (h)	500		

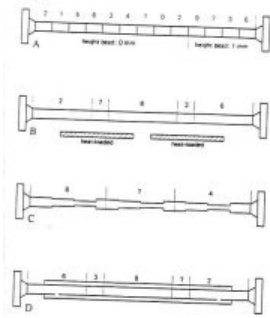


Figure 2. The four types of test tubes. The numbers refer to the steel composition.

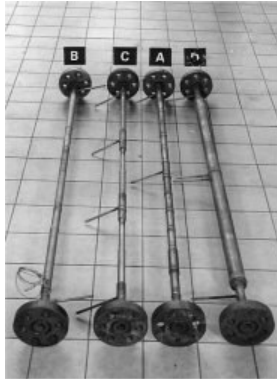


Figure 3. The four types of test tubes. Studs were mounted on tubes A, C and D in order to perform frequency measurements.

Various types of tubes were made for studying the influence of steel composition, heat load, thickness of the tube wall, and presence of a casing.

Tube type A

The German studies had not considered the influence of steel composition on rippling. Tubes were therefore made of nine steel types of different composition, all with identical inner and outer diameters. Most welds were made without beads inside by using gas counter-pressure in the tube. The chemical analysis of the steel types is given in Table 2.

Tube type B

The first experiment concerned the influence of heat load on a tube composed of five different steel types. On the basis of the results obtained during this experiment, it was decided to use simple one-material tubes (type E) for the heat-load conditions in the second experiment.

Tube type C

The thickness of the tube wall was expected to influence rippling. The hypothesis was that the tubes started vibrating because of the high water velocity.

The natural frequencies of the tube were therefore determined, for which purpose 15 cm long studs were welded onto tubes C, A and D (Fig. 3).

No clear differences were found between the individual tubes. Tube C was turned off to wall thicknesses of 7.5 and 3 mm respectively to study possible effects on rippling.

Tube type D

In the German study tubes of 13CrMo44 and 10CrMo910 were provided with a casing. In the KEMA study the inner tube was composed of five steel types: carbon steel, 15Mo3, 14Mn4, 13CrMo44 and 10CrMo910.

Table 2. Chemical composition (weight %) of steels involved in the KEMA study.

Steel type	Nr.	C	Mn	Si	P	S	Cr	Mo	Al	Cu	Ni
Carbon steel	0	0.08	0.50	0.18	0.012	0.012	0.06	0.01	0.02	0.04	0.04
	1	0.10	0.65	0.18	0.021	0.024	0.08	0.02	0.01	0.14	0.08
	2	0.10	0.48	0.25	0.009	0.026	0.03	0.01	0.01	0.10	0.04
15Mo3	3	0.16	0.59	0.24	0.004	0.022	0.04	0.26	0.01	0.10	0.06
	4	0.18	0.68	0.21	0.006	0.020	0.05	0.26	0.01	0.10	0.06
14Mn4	5	0.16	1.11	0.42	0.007	0.022	0.08	0.02	0.03	0.10	0.06
	6	0.16	1.09	0.25	0.020	0.032	0.03	0.01	0.01	0.12	0.06
13CrMo44	7	0.15	0.58	0.21	0.017	0.023	0.86	0.45	<0.01	0.06	0.03
10CrMo910	8	0.10	0.48	0.30	0.14	0.23	2.44	1.04	<0.01	0.10	0.24
	9	0.11	0.48	0.28	0.22	0.27	2.51	0.96	<0.01	0.12	0.09

3 Microscopic examinations

After the exposure test the tubes were cut longitudinally, in order to find the proper places for microscopic examination of the ripple structures. A large number of samples were taken for visual inspection and examination by means of a scanning electron microscope. In this paper only a limited number of photographs can be presented.

Ripple types

It appeared that there were two types of ripples: deposition ripples and erosion-corrosion ripples. Both types of rippling were more pronounced in the supercritical experiment than in the subcritical experiment. Microscopic examination showed that under supercritical conditions very clear erosion-corrosion ripples develop, whereas under subcritical conditions erosion-corrosion ripples are found only downstream from welds.

Deposition rippling

Loose magnetite crystals arrange themselves in the ripple structure because of the turbulent water flow over the tube surface. At places with low local water flow, coarse crystalline magnetite is present, whereas only fine crystalline magnetite is found in

the valleys where high water velocities occur. An example is given in Figure 4a, 4b and 4c.

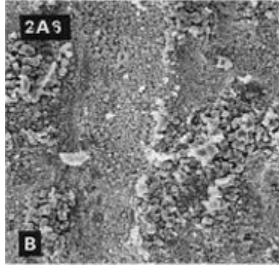


Figure 4a. Example of deposition rippling. Magnification 500 x.

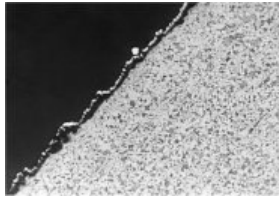


Figure 4b. Example of deposition rippling from a power station boiler. Cross section.

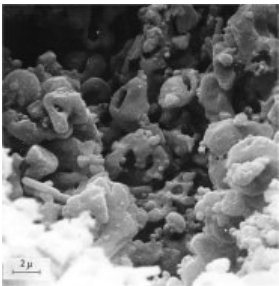


Figure 4c. Eroded magnetite crystals from the top of the deposition ripples in Figure

The magnetite for this type of rippling need not originate from the local steel surface itself. The oxide can also be supplied from other surfaces in the boiler and be deposited as ripples. This process is therefore called deposition.

Erosion-corrosion rippling

The steel surface corrodes and develops a ripple pattern because of local high and low water flows. Magnetite layers in the valleys are thin; those on the tops are thicker with coarser crystals. Examples are given in Figures 5 and 6.

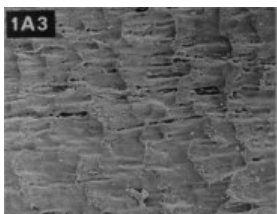


Figure 5. Erosion corrosion rippling patterns on steel 15Mo3 (magnification: x 100).

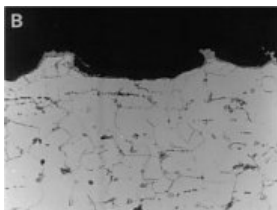


Figure 6. Rippling patterns on steel 15Mo3, downstream a weld bead (magnification: x 100), cross section.

Steel composition

Microscopic examination allowed an erosion-corrosion rippling ranking to be established for the steels. Very noticeable ripples were found with 15Mo3 and 14Mn4. Figure 6 shows that steel type 3 (15Mo3) was corroded in the valleys. The difference in oxide thickness between valleys and tops can be seen downstream from weld beads where turbulence enhanced rippling.

A less clearly noticeable rippling was found with carbon steels under supercritical conditions. Only steel type 0 showed erosion-corrosion ripples; some deposition rippling was found on steel type 2. None of the low-chromium steels (13CrMo44 and 10CrMo910) showed erosion-corrosion rippling but deposition ripples were present.

Heat load

Rippling was found in both experiments but the heat flux (300 kW/m²) apparently had no influence. Figure 7 shows erosion-corrosion rippling of 14Mn4 steel in the heat-loaded tube 1 B. The samples were taken from the heat-loaded and the non heat-loaded parts of the tube.

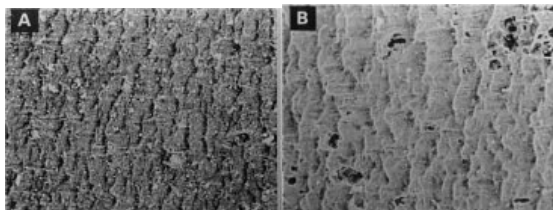


Figure 7. Erosion-corrosion rippling of heat-loaded (A) and non heat-loaded (B) specimens from 14Mn4 steel, specimen 1B6. Magnifications x 100.

Thickness of the tube wall

Tube-wall thickness did not affect rippling. Tube type C was made of steel types 15Mo3 (number 4), 13CrMo44 (number 7) and 10CrMo910 (number 8). Only deposition rippling was observed in those steels. Erosion-corrosion rippling was not found in 15Mo3 steel either.

Casing

Figure 8 shows that casing has a marked effect on rippling: the type of ripple changes with the casing. Erosion-corrosion rippling is found on the cased area (except for chromium-alloyed steels). Deposition rippling has developed outside that area.

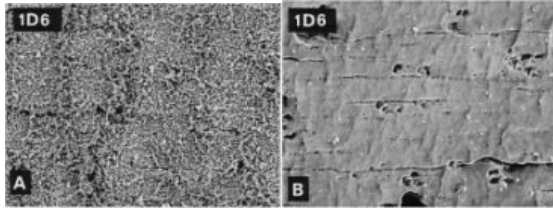


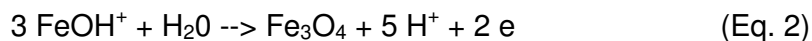
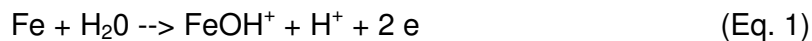
Figure 8. Rippling pattern in 14Mn4 (1D6). A: sample from cased tube (magnification x 100). B: sample from inside cased area. Deposition rippling in A (cased area) and erosion-corrosion rippling in B (outside cases=d area).

4. Discussion

A steel surface covered with a thin oxide layer suffers continuous 'corrosion'. The steel below the more or less porous oxide becomes corroded and FeOH^+ , HFeO_2^- or solved $\text{Fe}(\text{OH})_2$ are formed. Which iron corrosion product is formed will depend on the pH value of the water in the pores of the oxide layer. The corrosion products move to the water-oxide front, oxidize and precipitate to form magnetite octahedrons.

That process is conditioned at the water-oxide front by pressure, temperature, oxygen content, redox potential, pH and water-flow velocity. With strong turbulence the diffuse boundary layer will be thin, resulting in HFeO_2^- , $\text{Fe}(\text{OH})_2$ or FeOH^+ being rapidly carried away. Under these conditions the corrosion rate depends strongly on the Reynolds and Schmidt numbers (Vetter, 1967). All factors affecting this process will be considered in the prevention of rippling.

Erosion-corrosion rippling clearly seems to be an electrochemical process. The following anodic reactions are to be considered.



To achieve electrical equilibrium, one or more cathodic reactions take place, such as the hydrogen reaction, the oxygen and the hydrogen peroxide reactions or the copper-reduction reaction:



The main cathodic reaction is that of hydrogen reduction and recombination.

Origin of rippling

The hypothesis for erosion-corrosion rippling is as follows. The metal surface has spots with high and low water velocities, with thin and thick diffuse boundary layers respectively. The thinner the boundary layer, the more extensive the removal of iron corrosion products and the supply of oxidizing agents (H^+ , O_2 , H_2O_2 , Cu^+). This results in increased corrosion in places of high water velocities resulting in the formation of valleys in the steel surface. Iron corrosion products in solution easily oxidize to form magnetite octahedrons in places with low turbulence.

Solubility and iron content in the water are major factors in rippling. That can be concluded from differences found in the four tubes after the first experiment. Those tubes were placed in series in the boiler. The water velocity in the boiler tubes themselves and in the connecting tubes was much lower because of a larger tube diameter. The surfaces thus did not corrode and were covered with a protecting oxide layer. In the first two tubes tested (1A and 1B) clear erosion-corrosion rippling is present, but deposition rippling has developed in a more pronounced way outside the cased areas. The difference seems to be a result of a higher iron content in the water in tubes 1C and 1D because of erosion-corrosion of tubes 1A and 1B.

It is highly probable that in the cased area of tube 1D atomic hydrogen did not diffuse through the inner tube into the casing. There was water under high pressure on both sides of the inner tube and there was no driving force for diffusion. Consequently, when there is a casing the H_2 partial pressure in the inner tube can increase thus polarizing the cathodic reaction on the inner side of the inner tube. The corrosion potential remains low and passivation (precipitation and crystallization of magnetite) cannot take place. Because of the turbulence on the tube surface, there will be areas of high (valleys) and low (tops) corrosion rates, and erosion-corrosion rippling is the consequence. The corrosion products are removed with the running water and they oxidize and precipitate as magnetite on the non-cased area of the tube. That part of the tube is not polarized by the hydrogen reduction reaction and deposition rippling therefore is found there.

Influence of steel types

As was seen, the influence of steel composition on rippling was formerly little taken into account. KEMA research has now shown that especially minor differences in composition affect erosion-corrosion and corrosion resistance substantially (Huijbregts & Koetsier, 1981; Huijbregts, 1984). Erosion-corrosion resistance can be calculated with the regression equation:

$$R_{KEMA} = 0.61 + 2.43 Cr + 1.64 Cu + 0.3 Mo.$$

It is concluded from practical experience that the risk of erosion-corrosion damage is reduced if the R_{KEMA} value is higher than 1.0 (Huijbregts, 1984). The R_{KEMA} values for the unalloyed steels used in this study are given in Table 3; they range from 0.82 to 1.04.

For the erosion-corrosion rippling, no clear difference is noticed for the three carbon, the two 14Mn4 and the two 15Mo3 steel types, though the chemical compositions

point to some differences in erosion corrosion resistance. As was to be expected, the low alloyed 13CrMo44 and IOCrMo9 steel types are more resistant to erosion-corrosion ripple formation because of their relatively high chromium content. There are no differences in deposition rippling for the unalloyed and low-alloyed steel types under investigation. This kind of rippling depends more on the iron or oxide contents of the water and on flow conditions.

Though the experiments showed no influence of heat flux upon oxide deposition, it can be concluded from practical experience with boilers that heat load greatly affects deposit formation, and thus should somehow also affect rippling.

Table 3. Calculated erosion-corrosion resistance values R_{KEMA} for the unalloyed steels.

$$R_{KEMA} = 0.61 + 2.43 Cr + 1.64 Cu + 0.3 Mo.$$

Steel type	Number	R _{KEMA}
Carbon steel	0	0.82
	1	1.04
	2	0.85
15Mo3	3	0.95
	4	0.97
14Mn4	5	0.97
	6	0.88

Conclusions

Rippling is inherent to high water velocities in boiler tubes and it occurs with supercritical pressures in particular. Rippling, although less prominent, was also found with subcritical pressures and with double phase flows.

There are two types of rippling: erosion-corrosion rippling and deposition rippling. Erosion-corrosion rippling is found with low alloyed steel types such as carbon, 14Mn4 and 15Mo3 steel types in particular. 13CrMo44 and IOCrMo910 steel types do not show any clear erosion-corrosion. Deposition rippling is found on all steel types investigated.

Erosion-corrosion rippling can be well explained by electrochemical processes. The rate of formation of that type of rippling depends on the corrosion potentials on the surface of the tube. The corrosion potentials are determined by a number of factors such as pH, H₂, HO₂, and O₂ content, pressure, temperature and corrosion resistance of the steel.

Electrochemical measurements might allow a quantitative approach of the problem.

References

1. Huijbregts, W.M.M. 1984 Erosion-corrosion of carbon steel in wet steam - *Materials Performance* 23: 39-45.
2. Huijbregts, W.M.M. & J.E. Koetsier 1981 The resistance of unalloyed steel against erosion-corrosion in wet steam environments - In: *Metallic corrosion, Volume I; Proceedings of the 8th International Congress on Metallic Corrosion (Mainz, 1981)*: 62d-629.
3. Pfau, B., R. Heinsch, E. Hegele, D. Schulz & D. Thomson 1978 Abschlussbericht nr. 15 zum Teilprojekt B3 - Magnetitschutzschicht - Riffelrauhigkeit (1974-1978) - Sonderforschungsbereich (SFB, Universitat Stuttgart) 157; 292 PP.
4. Schoch, W., H. Wiehn, R. Richter & H. Schuster 1972 Magnetitbildung und Druckverlustanstieg in einem Besonkessel - VGB (Vereinigung der Grosskraftwerksbetreiber) *Kraftwerkstechnik* 52: 228-242.
5. Schuster, H. 1971 Magnetitbildung und Druckverlustanstieg im Verdampfer von Besonkesseln - *Allianz Berichte fur Betriebstechnik und Schadenverhutung* 16: 28-36.
6. Vetter, K.J. 1967 *Electrochemical kinetics* - Academic Press (London): 789 pp. + annexes.